Bioorganic & Medicinal Chemistry Letters 19 (2009) 1380–1385

Contents lists available at ScienceDirect

Bioorganic & Medicinal Chemistry Letters

journal homepage: www.elsevier.com/locate/bmcl

Quinolines as a novel structural class of potent and selective PDE4 inhibitors: Optimisation for oral administration

Christopher J. Lunniss *, Anthony W. J. Cooper, Colin D. Eldred, Michael Kranz, Mika Lindvall †, Fiona S. Lucas, Margarete Neu, Alex G. S. Preston, Lisa E. Ranshaw, Alison J. Redgrave, J. Ed Robinson, Tracy J. Shipley, Yemisi E. Solanke, Don O. Somers, Joanne O. Wiseman

GlaxoSmithKline Medicines Research Centre, Gunnels Wood Road, Stevenage, Hertfordshire SG1 2NY, England

ARTICLE INFO

Article history:
Received 28 November 2008
Revised 9 January 2009
Accepted 14 January 2009
Available online 19 January 2009

Keywords:
PDE4
Quinoline
Crystallography
COPD

ABSTRACT

Crystallography-driven optimisation of a lead derived from similarity searching of the GSK compound collection resulted in the discovery of a series of quinoline derivatives that were highly potent and selective inhibitors of PDE4 with a good pharmacokinetic profile in the rat. Quinolines **43** and **48** have potential as oral medicines for the treatment of COPD

The use of phosphodiesterase 4 (PDE4) inhibitors for the treatment of chronic obstructive pulmonary disease (COPD) is well documented in the scientific literature.[1–3] The current generation of PDE4 inhibitors, represented by Roflumilast (Daxas™) **1**, show moderate efficacy in COPD at tolerated doses, however, the maximum dose that can be given (and hence efficacy) is still limited by undesired side effects such as nausea and emesis.[4] Our objective was thus to develop an oral PDE4 inhibitor with improved therapeutic index.

The initial lead compound and start point was trisubstituted quinoline **2** (Fig. 1). This quinoline series was discovered from similarity searching for alternative templates to the original pyrazolopyridine template, for example, pyrazolopyridine **3** that was being worked on in GSK.[5] When the first co-crystal structure of a quinoline **4** bound in the active site of the PDE4B enzyme was solved, it was discovered that the quinoline series had a different binding mode to that of the pyrazolopyridine template and that the SAR did not transfer between the two series. An overlay of pyrazolopyridine **3** and quinoline **4** bound into the active site of the PDE4 enzyme is shown in Figure 2. It shows that the two amide moieties are binding into different parts of the active site and the two amine substituents are binding into the same pocket.

This letter describes the SAR that was discovered, culminating in the identification of two compounds that had the required profile to progress into our in-vivo models to evaluate their therapeutic index with respect to nausea and emesis.

Quinoline **2** has an attractive profile and is a good start point to initiate a lead optimisation programme. It has submicromolar activity against PDE4B ($pIC_{50} = 7.0$). It is greater than 300-fold selective against other PDE enzymes (PDE3 and PDE5) and has three potential points of diversity. It also has a low *c*log*P* (2.1) and moderate aqueous solubility (30 μg/mL). Unfortunately, quinoline **2** suffers from poor oral exposure in the rat. The primary emphasis of our SAR exploration was to increase the cellular activity and improve the rat oral pharmacokinetic (PK) profile. The biological profile that was targeted was: human whole blood (hWB) potency pIC_{50} >7.5 (inhibition of LPS induced TNFα production)[8]; >100-fold selective versus other PDEs; PK profile in the rat consis-

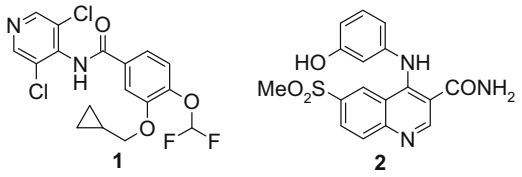

Figure 1. Structure of Roflumilast (**1**) and quinoline lead **2**. Profile of Roflumilast (**1**): PDE4B $pIC_{50} = 9.4$; >300-fold selective versus PDEs 3 and 5; hWB $pIC_{50} = 7.7$.

* Corresponding author. Fax: +44 (0)1438 768301.
E-mail address: christopher@lunniss.net (C.J. Lunniss).
† Present address: Novartis Institute for Biomedical Research, 4560 Horton Street, Emeryville, CA 74607, USA.

0960-894X/$ - see front matter © 2009 Elsevier Ltd. All rights reserved.
doi:10.1016/j.bmcl.2009.01.045

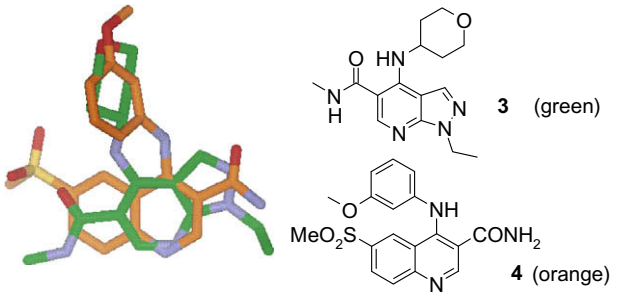

Figure 2. Overlay of pyrazolopyridine **3** and quinoline **4** bound in the active site of the PDE4B enzyme. Shown without the peptide for clarity.[6]

tent with once daily dosing ($F > 30\%$; $t_{1/2} > 2$ h). The PDE4 enzyme has four sub-types: A, B, C and D, but it is the PDE4B sub-type that is believed to play a central role in inflammation,[7] being the predominant subtype in monocytes and neutrophils and hence we used this isoform for routine screening. For the exemplars from this quinoline series tested against PDE4A, B, C and D, no isoform selectivity was observed.

The quinoline template can be assembled in five steps from commercially available starting materials in good overall yield (Scheme 1). 4-(Methylsulphonyl)aniline **5** was condensed with diethyl ethoxymethylenemalonate to give aniline derivative **6**. Cyclisation at 250 °C in diphenyl ether provided ester **7** which underwent basic hydrolysis to provide the 3-carboxylic acid quinolone derivative. Chlorination of the quinolone and quenching of the resultant acid chloride with aqueous ammonia, followed by displacement of the 4-chloro group in quinoline **8** with 3-hydroxyaniline in refluxing acetonitrile gave quinoline **2**.[9–11]

Modifications to the linker group at the 4 position were made by displacing the 4-chloro substituent in quinoline 8 (Scheme 2). The oxygen linker was introduced by displacement with a phenol and potassium carbonate in DMF. The sulphide linker was inserted by displacement with a thiol in refluxing acetonitrile with triethylamine.

Modifications to the primary carboxamide were made using standard functional group transformations (Schemes 3 and 4). The primary carboxamide **4** was converted to nitrile **11** using trifluoroacetic acid anhydride and subsequently hydrogenated to afford amine **12**. Quinolone ester **7** was reacted with thionyl chloride

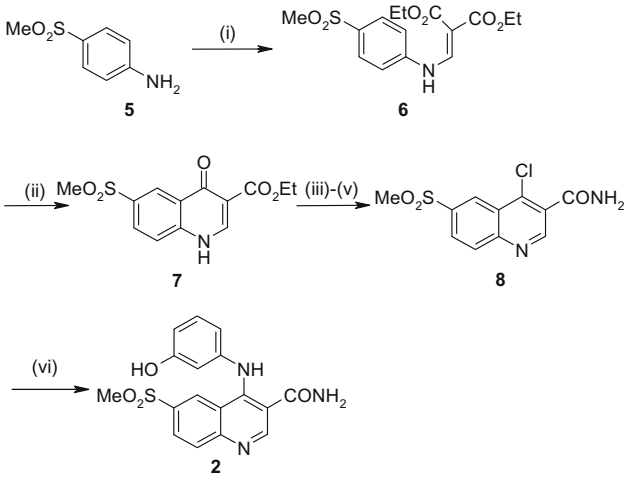

Scheme 1. Synthesis of quinoline **2**. Reagents and conditions: (i) Diethylethoxymethylenemalonate, 80 °C; (ii) Ph_2O, 250 °C; (iii) NaOH, EtOH; (iv) $SOCl_2$, DMF (cat); (v) NH_4OH; (vi) 3-hydroxyaniline, MeCN, 80 °C.

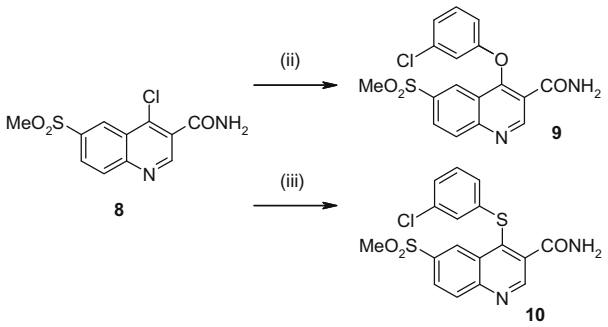

Scheme 2. Synthesis of compounds with variation of the R4 linker. Reagents and conditions: (ii) K_2CO_3, 3-chlorophenol, DMF; (iii) 3-chlorobenzenethiol, Et_3N, MeCN, 80 °C.

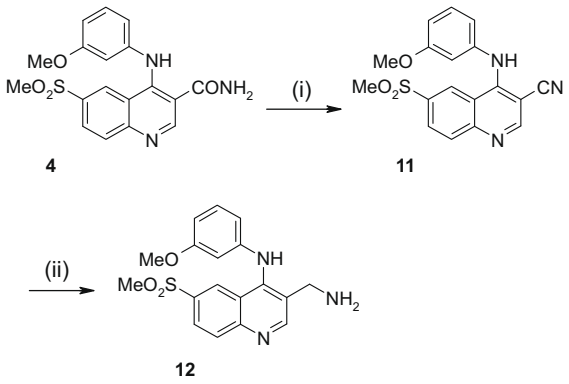

Scheme 3. Synthesis of quinolines with variation at the 3-position. Reagents and conditions: (i) TFAA: (ii) H_2, Pd/C, EtOH.

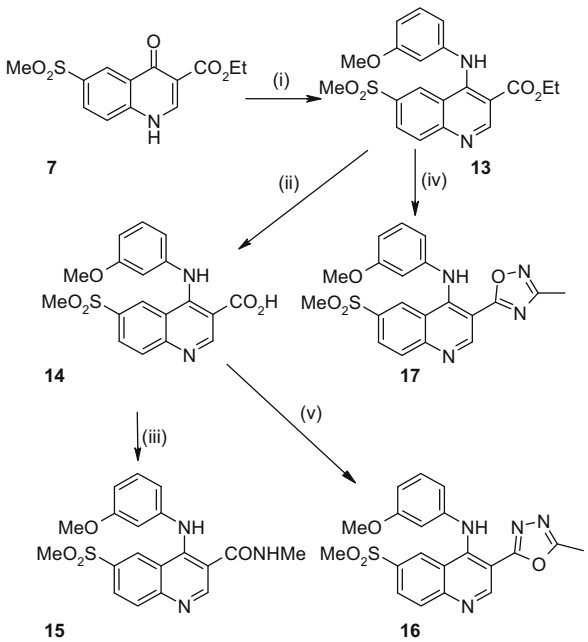

Scheme 4. Synthesis of quinolines with variation at the 3-position. Reagents and conditions: (i) $SOCl_2$, DMF, then 3-methoxyaniline, MeCN, 80 °C; (ii) NaOH, EtOH; (iii) TBTU, $^{i}Pr_2NEt$, amine, DMF; (iv) *N*-hydroxyethanimidamide, NaOEt, 3 Å molecular sieves, DMF, reflux; (v) $CH_3C(O)NHNH_2$, EDC, HOBT, DMF, followed by Burgess reagent, THF.

and then treated with 3-methoxyaniline in refluxing acetonitrile to give quinoline ester **13**. This ester was hydrolysed with sodium

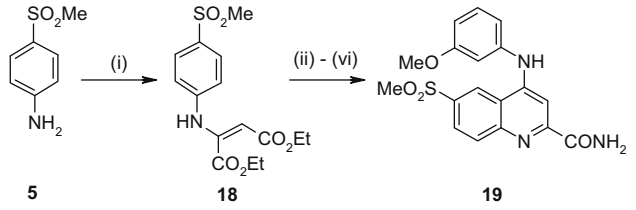

Scheme 5. Synthesis of 2-substituted quinolines. Reagents and conditions: (i) diethyl 2-butynedioate, 80 °C; (ii) Ph_2O, 250 °C; (iii) $SOCl_2$, DMF (cat); (iv) 3-methoxyaniline, MeCN, 80 °C; (v) NaOH, EtOH; (vi) TBTU, $^iPr_2NEt$, DMF, 0.880 ammonia.

hydroxide in ethanol to give acid **14**. Acid **14** was treated with TBTU in DMF followed by an amine to give amide **15**. Acid **14** was transformed into the 1,3,4-oxadiazole **16** by treatment with an acyl hydrazide followed by cyclo-dehydration with Burgess' reagent.[12] To form 1,2,4-oxadiazole **17,** ester **13** was reacted with *N*-hydroxyethanimidamide.

The synthesis of the compound with the primary carboxamide group moved to the 2-position of the quinoline is shown in Scheme 5. 4-(Methylsulphonyl)-aniline **5** was condensed with diethyl 2-butynedioate at 80 °C,[13] followed by similar chemistry to that which was used to prepare the 3-substituted analogues.

Variation of the 8-substituent was not possible at a late stage of the synthesis so modifications were made as shown in Scheme 6. Quinolines containing the 8-methyl and 8-methoxy substituents were synthesised by displacement of an aromatic fluoride **20** and **21** with sodium methane sulphinate at 75 °C in DMA,[14] followed by reduction of the nitro group to give amines **22** and **23**. The synthesis then proceeded as described in Scheme 1. Condensation of aryl iodides **24**–**27** with diethylethoxymethylene malonate and cyclisation in diphenyl ether at 250 °C followed by ester hydrolysis, chlorination with thionyl chloride and reaction with ammonia gave intermediates **28**–**31**. Amine displacement in refluxing acetonitrile followed by palladium-catalysed coupling with the tributyl(methylthio)stannane in refluxing toluene under palladium catalysis.[15] Oxidation with Oxone® afforded the target compounds.

Initially we investigated finding a replacement for the potentially metabolically vulnerable hydroxy substituent on the pendant aromatic ring in quinoline 2. As shown in Figure 2 the group at C-4 in the quinoline binds into the same part of the active site of the PDE4B enzyme as the cyclic substituents that gave potent compounds in the pyrazolopyridine series, such as the tetrahydopyran

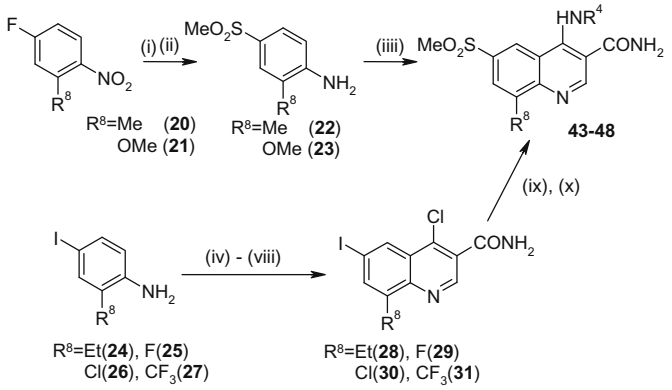

Scheme 6. Synthesis of variants at the quinoline 8-position. Reagents and conditions: (i) $MeSO_2Na$, DMA, 75 °C; (ii) Pd/C, H_2, AcOH; (iii) see conditions in Scheme 1; (iv) Diethylethoxymethylenemalonate, 80 °C; (v) Ph_2O, 250 °C; (vi) NaOH, EtOH; (vii) $SOCl_2$, DMF (cat); (viii) NH_4OH; (ix) amine, MeCN, 80 °C; (x) $MeSSnBu_3$, $Pd(PPh_3)_4$, toluene, reflux, then Oxone, DMF.

group (e.g., pyrazolopyridine 3 PDE4B pIC_{50} = 7.1).[16] Unfortunately, the quinoline **32** with the tetrahydropyran in the 4-position was inactive (Table 1). It was discovered that an aromatic substituent was essential for potency in this position in this quinoline series. Removal of the 4-substituent resulted in an inactive compound **33**.

A large number of compounds were synthesised investigating a wide range of substituents, a selection of which is detailed in Table 1. Some of the key SAR findings for PDE4B enzyme potency were:

- *Meta* substitution on the aromatic ring was preferred by the PDE4B-binding site.
- Large and bulky substituents in the ortho and para positions reduced PDE4B potency (data not shown).
- *Ortho* substitution with small substituents was tolerated (**34**, **35**, and **4**) especially if constrained in a ring to the meta position (**36**).
- Heterocyclic phenyl ring replacements and basic substituents reduced the log*P* (**37** *c*log*P* = 1.6 and **38** *c*log*P* = 1.4) which was potentially advantageous for oral exposure, but they were less potent at PDE4B.
- Acidic substituents on the phenyl ring were not well tolerated (**39**).

The replacement of the metabolically vulnerable hydroxy group in quinoline **2** by a methoxy group **4** resulted in an increase in potency and an improved rat PK profile giving 10% oral bioavailability. Further improvements in the PK profile were observed by replacing the methoxy group with a nitrile **35** or constraining the methoxy group into a ring as in the dihydrobenzofuran **36**. The addition of fluorine (**40** and **41**) onto the aryl ring resulted in improved bioavailability.

Modifications to the 4-amino linker group were very detrimental to PDE4B potency (Table 2).

This data indicates the potential importance of an intramolecular hydrogen bond between the NH and the carbonyl group of the 3-carboxamide. This hydrogen bond is not possible with any of the other linkers that were tried, possibly contributing to their lack of PDE4B binding potency.

Next the hydrogen bond donor/acceptor properties of the primary carboxamide were modified, small substituents placed on the nitrogen (**11**, **12a**, **14a** and **15**) and the primary carboxamide replaced with simple aromatic heterocycles (**16** and **11**). Some of the compounds described in Table 3 have a phenyl sulphone group in the 6-position of the quinoline (e.g., **4a**, **12a** and **14a**). This group was under investigation as an inhaled target early in the programme. The phenyl sulphone gave a higher PDE4B enzyme potency compared to the methyl sulphone, but was detrimental for solubility and oral PK.[19] The chemistry to make the compounds with the phenyl sulphone is analogous to the chemistry to make compounds with the methyl sulphone. All of these modifications reduced the potency at PDE4B significantly (Table 3). These data showed that the 3-primary carboxamide was essential for the high binding affinity of the quinolines in the PDE4B enzyme. This was rationalised when the crystal structure of **4** bound to the catalytic domain of PDE4B was determined (Fig. 3).

The primary carboxamide sits in a small binding pocket with one of the NH's hydrogen bonding to asparagine-395 in PDE4B and the other NH binding to glutamine-443 via a water molecule (Fig. 3). The carbonyl group participates in two hydrogen bonds, one to the NH of the 4-amino group and a second to an extensive water network. The intra-molecular hydrogen bond is believed to lock the quinoline into the preferred conformation to bind into the active site of the PDE4B enzyme.

The crystal structure of quinoline **4** bound in the active site of the PDE4B enzyme showed the presence of a small lipophilic binding pocket beneath the 8-position of the quinoline (Fig. 4). Subse-

Table 1
PDE4B, hWB potency and rat PK profile of compounds modifying the 4-amino substituent[8,17,18]

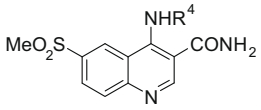

	R4	PDE4B pIC_{50} (n)	hWB pIC_{50} (n)	Rat F%	$t_{1/2}$ (h)	Cl (mL/min/kg)	Solubility (μg/mL)
2	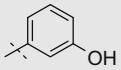	7.0 (6)	—	—	—	—	30
4	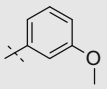	8.4 (7)	—	10	1.1	10	5
32		<4.5 (1)	—	—	—	—	—
33	H	<4.5 (1)	—	—	—	—	—
34	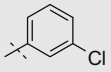	7.8 (3)	6.6 (4)	—	—	—	2
35	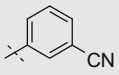	7.7 (4)	6.5 (8)	23	0.9	16	—
36	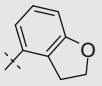	8.6 (2)	7.6 (4)	38	1.7	38	43
37		7.0 (1)	5.7 (2)	—	—	—	—
38	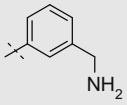	7.1 (1)	5.9 (2)	—	—	—	—
39	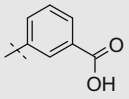	5.3 (1)	—		—	—	—
40	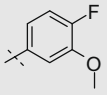	7.5 (5)	6.8 (4)	65	1.9	21	4
41	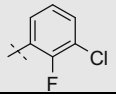	8.2 (2)	6.6 (4)	47	2.0	13	12

Table 2
PDE4B potency of compounds modifying the linker to the 4-substituent

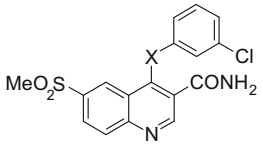

	X	PDE4B pIC_{50} (n)
9	O	5.5 (1)
10	S	4.7 (1)
34	NH	7.8 (3)
42	NMe	6.0 (1)

quently a range of small substituents in the 8-position of the quinoline were investigated.

The 8-methyl quinoline **43** was found to be 1.3 log units more potent than the unsubstituted compound in the hWB assay and it had an excellent PK profile in the rat (Table 4). Increasing the size of the 8-substituent to an ethyl or a chloro group (**44** and **45)** increased the potency in the enzyme assay (data not shown) but their increased lipophilicity resulted in a larger drop off into the cellular assay, resulting in compounds that were equipotent with the 8-methyl quinolines. The 8-chloro compounds suffered from a lack of oral exposure and this precluded their progression. 8-Fluoro analogue **46** was slightly less potent than 8-methyl quinoline **43** and consequently was not progressed. Methoxy derivative **47**

Table 3
PDE4B potency of compounds modifying the primary carboxamide

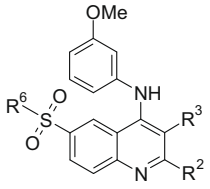

	R3	R2	R6	PDE4B pIC_{50} (n)
4	$-CONH_2$	H	Me	8.4 (7)
4a	$-CONH_2$	H	Ph	8.8 (2)
11	–CN	H	Me	6.3 (1)
12a	$-CH_2NH_2$	H	Ph	6.6 (1)
14a	$-CO_2H$	H	Ph	4.9 (1)
15	–CONHMe	H	Me	5.5 (1)
16		H	Me	4.7 (1)
17		H	Me	4.8 (1)
19	H	$-CONH_2$	Me	5.1 (1)

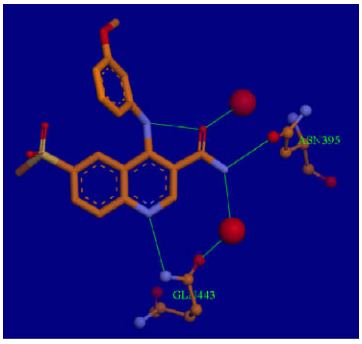

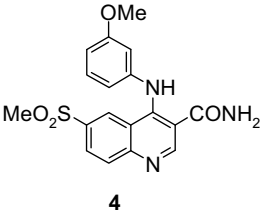

4

Figure 3. Picture of quinoline **4** in the PDE4B active site showing the hydrogen bond network around the primary carboxamide. Water is represented by red spheres. The green lines represent hydrogen bonds.

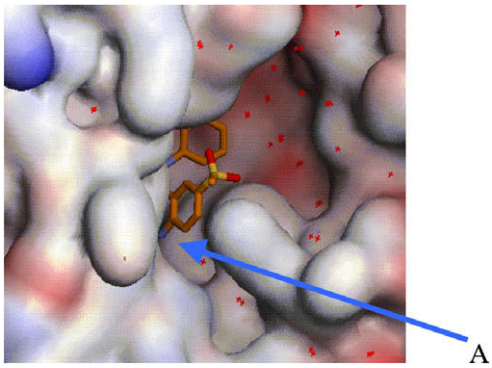

Figure 4. Crystal structure of quinoline **4** in the active site of the PD4B enzyme showing the small binding pocket (A) beneath the 8-position of the quinoline.

showed a reduction in potency that was rationalised by the 8-methoxy group being unfavorably twisted out of the plane of the quinoline ring to fit into the PDE4B-binding site.

In summary the quinoline series has been optimised to improve its potency and oral PK profile resulting in the discovery of key compounds **43** and **48** (Table 5).

Table 4
PDE4B, hWB potency and rat PK profile of compounds modifying the quinoline 8-substituent

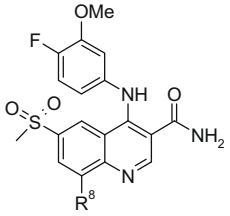

	R8	PDE4B pIC_{50} (n)	hWB pIC_{50} (n)	Oral AUC (ng h/mL)	F%	$t_{1/2}$ (h)	Cl (mL/min/kg)
40	H	7.5 (5)	6.8 (4)	530	65	1.9	21
43	Me	9.5 (3)	8.1 (10)	770	82	1.6	16
44	Et	–	7.9 (2)	–	–	–	–
45	Cl	–	8.1 (5)	16	–	–	–
46	F	–	7.8 (2)	–	–	–	–
47	OMe	8.3 (1)	6.6 (3)	81	–		

Table 5
Structure and profile of compounds **43** and **48**

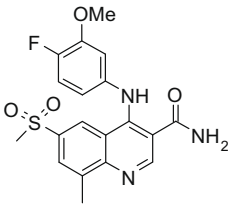

43

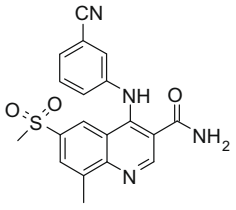

48

	PDE4B pIC_{50} (n)	hWB pIC_{50} (n)	F%	$t_{1/2}$ (h)	Cl (mL/min/kg)	$c\log P$	Solubility (μg/mL)
43	9.5 (3)	8.1 (10)	82	1.6	16	3.1	5
48	9.4 (2)	7.6 (11)	27	2.3	19	3.5	18

These compounds are very potent inhibitors of PDE4B, they are >100-fold selective over other PDEs (PDE1, 2, 3, 5, 6 and 7), have some aqueous solubility, a reasonable $c\log P$ and have a good PK profile in the rat. They were progressed to our in-vivo models for further profiling to determine a therapeutic index versus emetic side effects and these results will be reported in due course.

Acknowledgments

The authors thank Magali Gillet, Fanny Loustau-Chartez and Lucie Krzackowski for their synthetic contributions whilst on placement at GSK.

References and notes

1. (a) Krishna, G.; Sankaranarayanan, V.; Chitkara, R. K. *Exp. Opin. Invest. Drugs* **2004**, *13*, 255; (b) Kodimuthali, A.; Jabris, S. S. L.; Pal, M. *J. Med. Chem.* **2008**, *51*, 5471.
2. (a) McKenna, J. M.; Muller, G. W. *Cyclic Nucleotide Phosphodiesterases in Health and Disease* **2007**, 667; (b) Dyke, H. J. *Exp. Opin. Ther. Patents* **2007**, *17*, 1183; (c) Smith, V. B.; Spina, D. *Curr. Opin. Invest. Drugs* **2005**, *6*, 1136.
3. Huang, Z.; Mancini, J. A. *Curr. Med. Chem.* **2006**, *13*, 3253.
4. Rabe, F.; O'Donnell, D.; Muir, F., et al *Eur. Resp. J.* **2004**, *24*, 267.
5. Kranz, M. J.; in preparation.
6. Methods as described in Ref.16, except compound **4** was soaked into an apo-PDE4B crystal at 0.25 mM for ~16 h. The final R-factor and R-free achieved for the refined crystal structure of complex **4** were 20.9% and 24.3%, respectively, and the coordinates deposited in the PDB as entry 3FRG.
7. Wang, P.; Wu, P.; Ohleth, K. M.; Egan, R. W.; Billah, M. M. *Mol. Pharmacol.* **1999**, *56*, 170.

8. Inhibition of LPS induced TNF-α production from whole blood using IGEN technology was carried out as described in Patent WO2007036733.
9. All compounds were characterised by LC/MS and ^{1}H NMR analysis.
10. Preparation of quinoline derivatives as phosphodiesterase inhibitors; WO2004103998.
11. Gould, R. g., Jr.; Jacobs, W. A. *J. Am. Chem. Soc.* **1939**, *61*, 2890.
12. Atkins, G. M.; Burgess, E. M. *J. Am. Chem. Soc.* **1968**, 4744.
13. Edmont, D.; Rocher, R.; Plisson, C.; Chenault, J. *Bioorg. Med. Chem. Lett.* **2000**, *10*, 1831.
14. Ulman, A.; Urankar, E. *J. Org. Chem.* **1989**, *54*, 4691.
15. Dickens, M. J.; Gilday, J. P.; Mowlem, T. J.; Widdowson, D. A. *Tetrahedron* **1991**, *47*, 8621.
16. Hamblin, J. N.; Angell, T. D. R.; Ballantine, S. P.; Cook, C. M.; Cooper, A. W. J.; Dawson, J.; Delves, C. J.; Jones, P. S.; Lindvall, M.; Lucas, F. S.; Mitchell, C. J.; Neu, M. Y.; Ranshaw, L. E.; Solanke, Y. E.; Somers, D. O.; Wiseman, J. O. *Bioorg. Med. Chem. Lett.* **2008**, *14*, 4237.
17. The ability of compounds to inhibit catalytic activity at PDE4B (human recombinant), PDE3 (from bovine aorta) and PDE5 (human recombinant) was determined by Scintillation Proximity Assay (SPA) in 96-well format as described in WO2004024728.
18. The pharmacokinetic parameters in male CD Sprague rats were determined following intravenous and oral administration at 1 mg/kg. Compound was administered as a solution in 10% DMSO: 90% PEG200 in Water (70:30 mix). Blood was collected over a 12-h time period. Plasma was prepared following centrifugation and compound extracted from 50 μL plasma using protein precipitation with acetonitrile. Samples were then evaporated under nitrogen and re-suspended in 100 μl of 25:75 acetonitrile/water. Analysis was performed using LC–MSMS with a 5-min fast gradient comprising 0.1% formic acid in water and 0.1% formic acid in acetonitrile (mobile phases), 20 μl injection volume, flow rate 4 mL/min and a LunaC18 column (5 cm × 2.1 mm, 5 μm) with detection on a Sciex API365 instrument. Pharmacokinetic data was generated using a non-compartmental approach.
19. Woodrow, M. D.; in preparation.